хвильову функцію, еквівалентну частинці. Виведене рівняння хвилі уникає проблем негативної енергії та ймовірності. Дається самоузгоджена класична інтерпретація хвильових явищ та гравітації.

Ключові слова: квантова хвиля, кватерніонна алгебра, рівняння Клейна-Гордона, гравітація.

Одержано редакцією 08.08.2017 Прийнято до друку 20.09.2017

УДК 621.78-978. 004.94 PACS 02. 05.12.31.36.37

A. Gokhman, D. Terentyev, M. Kondria

ISOCHRONAL ANNEALING OF ELECTRON-IRRADIATED TUNGSTEN MODELLED BY CD METHOD: INFLUENCE OF CARBON ON THE FIRST AND SECOND STAGES OF RECOVERING

The evolution of the microstructure of tungsten under electron irradiation and post-irradiation annealing has been modelled using a multiscale approach based on Cluster Dynamics simulations. In these simulations, both self-interstitials atoms (SIA) and vacancies, carbon atoms isolated or in clusters, are considered. Isochronal annealing has been simulated in pure tungsten and tungsten with carbon, focusing on recovery stages I and II. The carbon atom, single SIA, single vacancy and vacancy clusters with sizes up to four are treated as the mobile pieces. Their diffusivities as well as the energy formation and binding energies are based on the experimental data and ab initio predictions and some of these parameters have been slightly adjusted, without modifying the interaction character, on isochronal annealing experimental data. The recovery peaks are globally well reproduced. These simulations allow interpreting the second recovery peak as the effect of carbon.

Key words: Post-irradiation Annealing**,** Tungsten, Carbon Effect, Cluster Dynamics.

1. Introduction

Tungsten is one of the candidate materials for the plasma facing component of fusion reactors because of its high melting point, high sputtering resistivity, and high temperature strength. Numerous studies have explored the recovery processes of radiation-induced damage in tungsten. Residual electrical resistivity was commonly used as an index of the damage present in materials for the damage recovery study, resulting in the identification of the temperatures and activation energies for different annealing stages. To date, the physical mechanisms governing the damage recovery of tungsten are still controversial. The next progress in study of this phenomenon could be done by Cluster Dynamics (CD) and Adaptive Kinetic Monte Carlo (AKMC) simulations. In our paper CD is applied to simulate the kinetics of point defects in post-irradiation annealing tungsten after electron irradiation. Special attention to effect of carbon is devoted.

2. Discussion of model and input material parameters

The mean field isotropic model on the electron-irradiated and post-irradiation annealing of pure tungsten and tungsten with carbon is applied. Because the distance between point defects expected to be more great than size of them the frustration effect isn't considered. Hence, the CD model for bcc iron with chromium and carbon [1] was modified to study of tungsten with carbon system.

In additional, new CD code takes into account the conclusion [2] on the mobility of vacancy dimmer, V_2, vacancy cluster with size of three and four, V_3 and V_4.

The lattice parameter of tungsten, a_0, is taken of 3.1652 ^{o}A [3]; line dislocation density, ρ_d, of 10^{12} m^{-2} [4]; grain size, d, of 50μm; Burgers vector, b, of 2.74 ^{o}A [3]. Capture efficiency for vacancy and (self-interstitial atoms) by dislocation net, Z_v (Z_i) are taken 1(1.2) as in [1]. Recombination radius for all pairs: vacancy-SIA, carbon-SIA, carbon-vacancy, (vacancy-carbon)-vacancy, (vacancy-carbon)-carbon is taken the same and equal to 4.65°A (r_{rec} = 4.65°A) as in [1,5]. The migration energy of vacancy, E_{mv}, is taken of 1.5 eV according to experimental data [6]. The migration energy of di-vacancy, E_{m2v}, three-vacancy, E_{m3v}, and four-vacancy, E_{m4v}, is taken as 1.6, 1.7 and 1.8 eV, respectively. Vacancy pre-exponential factors for vacancy clusters and SIA, D_{v0}, D_{2V0}, D_{3V0}, D_{4V0} and D_{i0} are assumed to be of 2*10^{-8} m^2/s. The value of SIA migration energy, E_{mi}, of 0.013eV was calculated in [7]. In our study E_{mi} is taken as the fitting parameter to get the best reproduction of experimental data on recovery of tungsten. Formation energy of SIA is taken of 9.466 eV according to [5]. Temperature dependence of carbon diffusivity into tungsten has been studied experimentally and theoretically in [8-12]. Following to data [8-12], pre-exponential factor, D_{C0}, and migration energy of carbon in tungsten, E_{cm}, are taken in our study as 2*10^{-8} m^2/s and 1.7eV. Value of surface energy, γ, is taken of 3.119 J/m^2, which is between calculated values [13]: γ = 2.275 J/m^2 for the crystallographic plane (100) and 3.221 J/m^2 for the crystallographic plane (110). Values of binding energy of SIA dimmer, E_{bi}, pairs SIA-carbon, E_{bic}, vacancy-carbon, E_{bvc}, (vacancy-carbon)-vacancy, E_{bvcv}, and (vacancy-carbon)-carbon, E_{bvcc}, are assumed to be 2.2, 1.15, 2.3, 2.3 and 2.3 eV, respectively. For comparison we present here some calculated literature data:

E_{bi} = 2.12eV [14]; E_{bvc} = 1.93 eV [12] and 1.39eV in [15].

3. Master Equation of CD simulations

Master Equation of CD simulations for both electron irradiation and post-irradiation annealing of tungsten is written by the system of ordinary differential equations for concentrations of vacancies (SIA$_s$) (Eqs. 1-3) and carbon - point defects complexes (Eqs. 4-7):

$$\begin{aligned}
&\frac{dC_{1v(i)}}{dt} = G_{dpa} - \frac{4\pi\, r_{rec}(D_v + D_i)C_{1v}C_{1i}}{\Omega_W} - \frac{4\pi\, r_{rec}(D_c + D_i)C_c C_{1iv(i)}}{\Omega_W} \\
&- \rho_d Z_v \left(1 + \frac{6\left(\rho_d Z_v\right)^{-0.5}}{d}\right) D_{v(i)}\left(C_{1v(i)} - C^e_{1v(i)}\right) - 4\beta^{v(i)}_{1v(i)} C_{1v(i)} + 4\alpha^{v(i)}_{2v(i)} C_{2v(i)} - \sum_{n=2} \beta^{v(i)}_{nv(i)} C_{nv} \\
&+ \sum_{n=3} \alpha^{v(i)}_{mv(i)} C_{nv(i)} + \beta^{i(v)}_{2v(i)} C_{2v(i)} - \sum_{n=2} \beta^{v(i)}_{ni(v)} C_{ni(v)} \\
&- \frac{4\pi\, r_{rec}(D_c + D_{v(i)})}{\Omega_W} \cdot \left(C_c C_{1v(i)} - \left(C_c + C_{v(i)}\right)\exp\left(-\frac{E_{bcv(i)}}{k_B T}\right)\right) - \\
&k_v \cdot \frac{4\pi\, r_{rec} D_v C_{1v} C_{vc}}{\Omega_W}\left(1 - \exp\left(-\frac{E_{bvcv}}{k_B T}\right)\right)
\end{aligned} \tag{1}$$

$$\frac{dC_{2v(i)}}{dt} = 2\beta_{1v(i)}^{v(i)} C_{1v} - 2\alpha_{2v(i)}^{v(i)} C_{2v(i)} - \beta_{2v(i)}^{v(i)} C_{2v(i)} + \alpha_{3v(i)}^{v(i)} C_{3v} - \beta_{2v(i)}^{i(v)} C_{2v} + \beta_{3v(i)}^{i(v)} C_{3v(i)} \quad (2)$$

$$\begin{aligned} &\frac{dC_{nv(i)}}{dt} = \beta_{(n-1)v(i)}^{v(i)} C_{(n-1)v(i)} + \left(\beta_{(n+1)v(i)}^{i(v)} + \alpha_{(n+1v(i))}^{v(i)}\right) C_{(n+1)v(i)} \\ &-\left(\beta_{nv(i)}^{v(i)} + \beta_{nv(i)}^{i(v)} + \alpha_{nv(i)}^{v(i)}\right) C_{nv(i)} \quad for \quad n > 2 \end{aligned} \quad (3)$$

$$\frac{dC_{vcc}}{dt} = \frac{4\pi\, r_{rec} D_c}{\Omega_W} \cdot C_c \cdot C_{vc} \left(1 - \exp\left(-\frac{E_{bvcc}}{k_B T}\right)\right) \quad (4)$$

$$\frac{dC_{vcv}}{dt} = \frac{4\pi\, r_{rec} D_v}{\Omega_W} \cdot C_v \cdot C_{vc} \left(1 - \exp\left(-\frac{E_{bvcv}}{k_B T}\right)\right) \quad (5)$$

$$\begin{aligned} \frac{dC_{ic}}{dt} = &\frac{4\pi\, r_{rec}\left(D_c + D_i\right)}{\Omega_W} \cdot \left(C_c C_i - \left(C_c + C_i\right) \exp\left(-\frac{E_{bic}}{k_B T}\right)\right) - \\ &\frac{4\pi\, r_{rec} D_c}{\Omega_W} \cdot C_c \cdot C_{vc} \left(1 - \exp\left(-\frac{E_{bvcc}}{k_B T}\right)\right) \end{aligned} \quad (6)$$

$$\begin{aligned} \frac{dC_{vc}}{dt} = &\frac{4\pi\, r_{rec}(D_c + D_{v(i)})}{\Omega_W} \cdot \left(C_c C_{1v(i)} - \left(C_c + C_{v(i)}\right) \exp\left(-\frac{E_{bcv(i)}}{k_B T}\right)\right) - \\ &\frac{4\pi\, r_{rec} D_v\, C_{1v} C_{vc}}{\Omega_W} \left(1 - \exp\left(-\frac{E_{bvcv}}{k_B T}\right)\right) \end{aligned} \quad (7)$$

Here G_{dpa} is electron flux, which equal to ratio of irradiation exposure (in dpa) to irradiation time for the case of electron irradiation and zero for the case of post-irradiation annealing, k_v is equal to one for vacancy and zero for SIA, $D_v\left(D_i\right) = D_{v(i)0} \cdot \exp\left(-\frac{E_{mv(i)}}{k_B T}\right)$ is the diffusivity of free vacancy (SIA), $\Omega_W = \frac{a_0^3}{2}$ is the atomic volume of tungsten, $C_{1i}\left(C_{1i}\right)$ is the concentration of free vacancies (SIA_s), $C_{1v(i)}$ is the thermal equilibrium vacancy (SIA) concentration, $C_{nv(i)}$ is the concentration of vacancy (SIA) clusters contain of n vacancies (SIA_s), C_{vc} is the concentration of vacancy-carbon pairs, C_{vcc} and C_{vcv} are the concentration of (vacancy-carbon)-carbon and (vacancy-carbon)-vacancy complexes; $\beta_{nv(i)}^{v(i)}$ and ($\alpha_{mv(i)}^{v(i)}$) are the absorption and emission coefficients of vacancies V, V_2, V_3 and V_4 (SIA) from VC (SIAC), which are calculated similar to [1].

The system of Equations (1-7) describes:

(1) formation of free vacancy and SIA due electron irradiation;
(2) vacancy - SIA recombination;
(3) trapping of vacancy (SIA) by dislocation net;
(4) trapping of vacancy (SIA) by carbon;
(5) vacancy (SIA) – recombination;
(6) absorption of vacancy (SIA) by vacancy cluster (VC) and SIA cluster (SIAC);
(7) emission of vacancy and SIA from VC and SIAC, respectively;
(8) absorption (emission) of VC with two, three and four vacancies by (from) VC;
(9) absorption (emission) of carbon or vacancy by (from) vacancy-carbon complex.

4. Cluster Dynamics simulations

Because the evolution of point defect system in post-irradiation annealed tungsten is the set of kinetics processes with the different characteristic times, the integration of the Master Equation (1-7) is the typical problem of stiff ordinary differential equations. Stiff equation is a differential equation for which classical numerical methods for solving the equation are numerically unstable, unless the step size is taken to be extremely small. Hence, the FORTRAN subroutine package, *LSODE*, the Livermore Solver for Ordinary Differential Equations [16] based on the backward differentiation formula method [17] has been taken as a main program of computer code. Following to [18], the electron irradiation exposure, irradiation time and irradiation temperature are taken as 0.0001 dpa, 43200 seconds and 5 K; the temperature step of isochronal annealing is taken about 5 K, the time of annealing on each step is taken 300 seconds for temperature below 450 K and about 600 seconds for temperature from 450 K to 500 K. CD simulations have been done for the initial concentration of free carbon atoms in tungsten about 100 ppm and for tungsten free from carbon.

It was found that electron irradiation of 0.0001 dpa during 43200 seconds at temperature of 5 K results in formation of Frenkel pairs with concentration about 100 ppm in both pure tungsten and tungsten with carbon. The increase of E_{mi}, to 0.163eV provided the quite good correspondence between experimental data [18] and simulation data in our study. Calculated by CD temperature dependences of concentration of free and clustering vacancies and SIAs; free carbon atoms, vacancy-carbon, SIA-carbon, VC-V and VC-V complexes in the post-irradiation annealed tungsten are presented on Figures (1-3). For the temperature range of isochronal annealing from 4.2 to 100 K (Stage I of the recover spectrum of tungsten [18]), we observe:

(1) decrease of the concentration of free vacancies to value about 29 ppm (57 ppm) for pure tungsten (tungsten with carbon) and of free SIA to zero for both pure tungsten (tungsten with carbon), formation of SIA clusters (SIAC) with concentration of clustering SIA about 21 ppm (10.6 ppm) for pure tungsten (tungsten with carbon), no vacancies clusterization for both pure tungsten (tungsten with carbon) in the temperature range from 55 to 100 K;

(2) formation of carbon-SIA pairs with concentration about 43 ppm and decrease of free carbon atoms to value about 57 ppm for tungsten with carbon in the same temperature range;

(3) no formation of vacancy-carbon, (vacancy-carbon)-vacancy and (vacancy-carbon)-carbon.

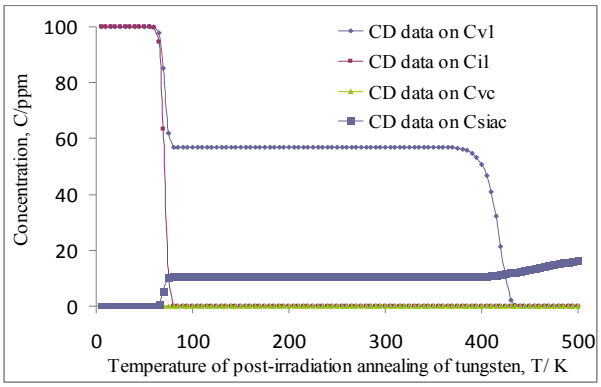

Figure 1. Temperature dependence of concentration of free vacancies (C_{v1}), free SIA$_s$ (C_{i1}), clustering vacancies into VC (C_{vc}) and clustering SIA into SIAC (C_{siac}) in post-irradiation annealing tungsten.

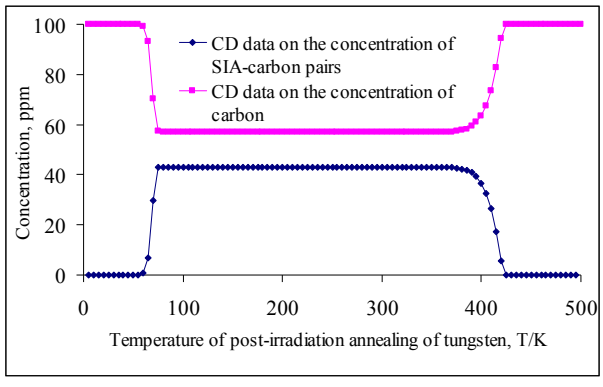

Figure 2. Temperature dependence of concentration of SIA-carbon pairs and carbon in post-irradiation annealing tungsten.

With aim to compare our CD results with experimental data [18], the differential isochronal resistivity recovery has been calculated on Equation (8) according to [18,19]:

$$100\% \bullet \frac{(\rho - \rho_0)/\rho_0}{LnT - LnT_0} = 100\% \bullet \frac{(n - n_0)/n_0}{LnT - LnT_0} \quad (8)$$

Here ρ and ρ_0 are the specific electrical resistivities; n and n_0 are the total number of Frenkel pairs at temperatures T and T_0. It was found that our CD simulations reproduce well the recovery peak centered at about 70 K (Fig. 4).

For the temperature range of isochronal annealing from 100 to 500 K (Stage II of the recover spectrum [18]), is observed in CD simulations:

(1) decrease of the concentration of free vacancies to zero, no significant changes of concentration of free SIA, clustering vacancies and SIA for the tungsten with carbon in the temperature range from 360 to 500 K;

(2) decrease of the concentration of carbon-SIA pairs to zero, increase of concentration of carbon atoms to 100 ppm, for the tungsten with carbon in the same temperature range;

(3) no significance change of concentrations of point defects for pure tungsten;

(4) very slight increase of concentration of vacancy-carbon, (vacancy-carbon)-vacancy and (vacancy-carbon)-carbon.

It was found that our CD simulations result in the recovery peak centered at about 420 K for the tungsten with carbon and no recovery peak for pure tungsten (Fig. 4).

Latter confirms the hypothesis of [18] on the role of impurities as traps for point defects on the Stage II.

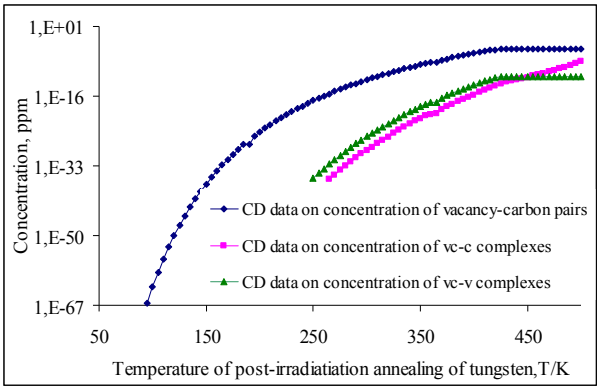

Figure 3. Temperature dependence of concentration of vacancy-carbon pairs, vc-c and vc-v complexes in post-irradiation annealing tungsten.

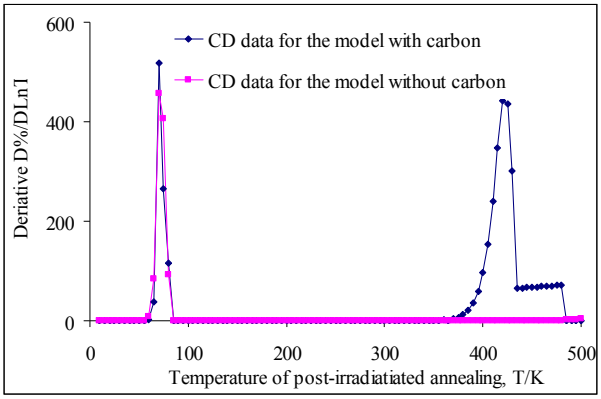

Figure 4. Derivative versus temperature plot of the irradiation recovery data for post-irradiation annealing tungsten.

5. Discussion

The first-order process attributed to recombination of a particularly close SIA-vacancy pair and the second-order process attributed to extensive diffusion of one of these defects, presumably SIA are discussed in [18] to reveal the physical nature of the peak centered about 70K at the Stage I. The conclusion on the mixture of the both first-order and second-order processes with dominating of the second-order process is done in [18]. It corresponds to the recombination of SIA-vacancy pairs and to self-trapping of SIA (formation of $SIAC_s$) and to trapping of SIA by impurities and some immobile sinks but the nature of them is not revealed in [18].

Let's consider the results of our CD simulation, which complement data [18]:

(1) All point defects are immobile under post-irradiation annealing in the temperature range from 5 to 50K

(2) Values of C_{v1} and C_{i1} are about of 53 and 0 ppm, respectively, for annealing temperature of 100K. Concentration of free vacancies fall downs slowly than SIA at the Stage I. It shows that recombination of SIA-vacancy pair isn't alone process and hence the first-order process doesn't attribute to this Stage.

(3) Values of concentration of SIA_s clustering into $SIAC_s$ and SIA-carbon pairs about 10.5 ppm and 43.0 ppm, respectively, for annealing temperature of 100K. With taking into account that concentration of C_{v1} decreases on 47 ppm, it means that at least 7.5 ppm C_{v1} are trapped by immobile sink, which is dislocation net.

There is a set of observed experimental small recovery peaks [18], which are not reproduced in our CD simulations. The possible reason is the paucity of data points in any of the apparent peaks in the Stage II region, which prohibits meaningful speculation concerning the shape of these peaks [18].

Next CD simulations will describe the stage III of recovering tungsten [18] need in new set of material parameters for the corresponding temperature diapason: 500-1000K.

6. Conclusion

1. We have shown how CD simulations reproduce well Stages I and II of the isochronal resistivity recovery experiment of electron-irradiated tungsten.
2. The carbon doesn't effect on the position of the recovery peak centered about 70K (Stage I) in tungsten with carbon.
3. The taking into account of the carbon presence needs to reveal the reason of recovery peak at the Stage II in tungsten with carbon.

Acknowledgements

This work was supported by the project "Development of theory for radiation damage in W-based alloys for fusion application".

References (in language original)

1. Gokhman A. Simulation of nanostructure evolution under helium implantation in Fe-(2.5-12.5)at% Cr alloys at temperature of 343K / A. Gokhman, S. Pecko and V. Slugeň // Radiation Effects and Defects in Solids: Incorporating Plasma Science and Plasma Technology – 2015. – Vol. 170 –P . 745-757.

2. Fu C. C. Multiscale modelling of defect kinetics in irradiated iron/ C. C. Fu, J. Dalla Torre, F. Willaime, J.L. Bocquet, A. Barbu // Nature Materials– 2005. – Vol. 4 – P. 68-74.

3. Fikar J. / J. Fikar, R. Schaublin // Nucl. Instr. Methods Phys. Res. – 2009. – Vol. B 267. – P. 3218–3222.

4. Dieter G. E. Mechanical Metallurgy / G. E. Dieter. – London, symmetric edition. : McGraw-Hill Book Company, 1988. – 352p.

5. Li Y. G. / A Cluster Dynamics Model for Accumulation of Helium in Tungsten under Helium Ions and Neutron Irradiation/ Y. G. Li, W. H. Zhou, R. H. Ning, L. F. Huang, Z. Zeng1, X. Ju // Commun. Comput. Phys . – 2012. – Vol. 11. – P. 1547-1568

6. Satta A. / Vacancy self-diffusion parameters in tungsten: Finite electron-temperature LDA calculations / A. Satta, F. Willaime, Stefano de Gironcoli // Phys. Rev. – 1998. – Vol. B 57 – P. 11184.

7. Derlet P. M. , Multiscale modeling of crowdion and vacancy defects in body-centered-cubic transition metals/ P. M. Derlet, D. Nguyen-Manh, S. L. Dudarev // Phys. Rev. – 2007. – Vol. B 76. – P. 054107

8. Withop, Arthur (1966). The diffusion of carbon into tungsten (PhD Thesis, The University of Arizona, the United States).

9. Aleksandrov L. N. / L. N. Aleksandrov // Zavodskaya Laboratorlya. – 1960. – Vol. 25. – P. 925-935.

10. Becker, J. A., E. I. Becker, and Re. G. Brandes // J. Appl. Phys. – 1961. – Vol. 32. – P. 411-423.

11. Bushmer C. P. Carbon Self-Diffusion in Tungsten Carbide/ C. P. Bushmer, P. H. Crayton // Journal of Material Science– 1971. – No 6 – P. 981-988.

12. Liu Yue-Lin. Dissolution and diffusion properties of carbon in tungsten / Yue-Lin Liu, Hong-Bo Zhou, Shuo Jin, Ying Zhang, Guang-Hong Lu // J. Phys. – 2010. – Vol. 22 – P. 445504 (6pp).

13. Tyson W. R. Surface free energies of solid metals: Estimation from liquid surface tension measurements, Surface Science / W. R. Tyson, W. A. Miller // Surface Science. – 1977. – Vol. 62 – P. 67-276.

14. Becquart C. S., C. Domain, U. Sarkar, and et al. // J. Nucl. Mater. – 2010 – Vol. 403 – P. 75 -88.

15. Nguyen-Manh D. Ab-initio Modelling of Point Defect-Impurity Interaction in Tungsten and other Bcc Transition Metals/ D. Nguyen-Manh // Advanced Materials Research – 2009. – No 59 – P. 253-256.

16. LSODA is part of the ODEPACK provided by Alan C. Hindmarsh 1984 on the CASC server of the Lawrence Livermore National Laboratory, Livermore, CA 94551, USA.

17. Gear C.W. Numerical Initial Value Problems in Ordinary Differential Equations / C.W. Gear– NJ. : . Prentice-Hall,Englewood Cliffs, 1971

18. Neely H. H. Keeper and A. Sosin, Electron Irradiation and Recovery of Tungsten / H. Neely, D. W. Keeper, A. Sosin // Phys. stat. sol. – 1968. – Vol. 28. – P. 675-682.

19. Ngayam-Happy R. Isochronal annealing of electron-irradiated dilute Fe alloys modelled by an ab initio based AKMC method: Influence of solute–interstitial cluster properties / R. Ngayam-Happy, P. Olsson, C. S. Becquart, C. Domain // Journal of Nuclear Materials. – 2010. –Vol. 407. – P. 16–28.

References

1. Gokhman A., Pecko S. and Slugeň V. (2015). Simulation of nanostructure evolution under helium implantation in Fe-(2.5-12.5)at% Cr alloys at temperature of 343K. *Radiation Effects and Defects in Solids: Incorporating Plasma Science and Plasma Technology. Vol. 170 –P . 745-757.*

2. Fu C. C., Dalla Torre, Willaime F., Bocquet J.L., Barbu A.. (2005). Multiscale modelling of defect kinetics in irradiated iron. *Nature Materials Vol. 4 – P. 68-74.*

3. Fikar J., Schaublin R.. (2009). *Nucl. Instr. Methods Phys. Res Vol. B 267. – P. 3218–3222.*

4. Dieter G. E. (1988). *Mechanical Metallurgy.* – London, symmetric edition. : McGraw-Hill Book Company (in England)

5. Li Y. G., Zhou W. H., Ning R. H., Huang L. F., Zeng Z., Ju X. (2012). Cluster Dynamics Model for Accumulation of Helium in Tungsten under Helium Ions and Neutron Irradiation. *Commun. Comput. Phys. Vol. 11. – P. 1547-1568*

6. Satta A., Willaime F., Stefano de Gironcoli. (1998). Vacancy self-diffusion parameters in tungsten: Finite electron-temperature LDA calculations. *Phys. Rev. Vol. B 57 – P. 11184.*

7. Derlet P. M., Nguyen-Manh D., Dudarev S. L., (2007). Multiscale modeling of crowdion and vacancy defects in body-centered-cubic transition metals. *Phys. Rev. Vol. B 76. – P. 054107*

8. Withop Arthur (1966).). *The diffusion of carbon into tungsten* (PhD Thesis, The University of Arizona, the United States).

9. Aleksandrov L. N. (1960). *Zavodskaya Laboratorya. Vol. 25. P. 925-935.*

10. Becker, J. A., E. I. Becker, and Re. G. Brandes. (1961). *J. Appl. Phys. Vol. 32. – P. 411-423.*

11. Bushmer C. P., Crayton P. H. (1971). Carbon Self-Diffusion in Tungsten Carbide. *Journal of Material Science No 6 – P. 981-988.*

12. Yue-Lin Liu, Hong-Bo Zhou, Shuo Jin, Ying Zhang, Guang-Hong Lu. (2010). Dissolution and diffusion properties of carbon in tungsten. *J. Phys. Vol. 22 – P. 445504 (6pp).*

13. Tyson W. R, Miller W. A. (1977). Surface free energies of solid metals: Estimation from liquid surface tension measurements. *Surface Science. Vol. 62 – P. 67-276.*

14. Becquart C. S., C. Domain, U. Sarkar, and et al. (2010). *J. Nucl. Mater. Vol. 403 – P. 75 -88.*

15. Nguyen-Manh D. (2009). Modelling of Point Defect-Impurity Interaction in Tungsten and other Bcc Transition Metals. *Advanced Materials Research No 59 – P. 253-256.*

16. LSODA is part of the ODEPACK provided by Alan C. Hindmarsh 1984 onthe CASC server of the Lawrence Livermore National Laboratory, Livermore, CA 94551, USA.

17. Gear C.W. (1971). Numerical Initial Value Problems in Ordinary Differential Equations. Gear– NJ. : Prentice-Hall,Englewood Cliffs. (in USA)

18. Neely H., Keeper D. W., Sosin A. (1968). Keeper and A. Sosin, Electron Irradiation and Recovery of Tungsten. *Phys. stat. sol. Vol. 28. – P. 675-682.*

19. Ngayam-Happy R., Olsson P., Becquart C. S., Domain C. (2010). Isochronal annealing of electron-irradiated dilute Fe alloys modelled by an ab initio based AKMC method: Influence of solute–interstitial cluster properties. *Journal of Nuclear Materials. Vol. 407. – P. 16–28*

Анотація. ***Гохман О., Терентьев Д., Кондря М. Ізохронний відпал електронно-опроміненого вольфраму, моделювання за методом кластерної динаміки: вплив вуглецю на першу і другу стадії відновлення.*** *Еволюція мікроструктури вольфраму під впливом електронного опромінення та після опромінюваного ізохронного відпалу була досліджена з використанням мультімасштабного підходу, який базується на моделюванні методом кластерної динаміки. У цих симуляціях розглядаються вільні точкові дефекти (міжвузельні атоми та вакансії), кластери точкових дефектів з розміром до 10000 мономерів, а також кластери, які складаються з атомів вуглецю та точкових дефектів. Зміна дефектної структури у процесі ізохронного відпалу вольфраму без домішків та вольфраму з вуглецем досліджується на першій стадії (температура ізохронного відпалу від 5 до 100 К) та другій стадії (температура ізохронного відпалу від 100 до 500 К) відновлення. Атоми вуглецю, вільні міжвузельні атоми, вільні вакансії та вакансійні кластери з розміром до чотирьох вакансій розглядаються як рухомі об'єкти, дифузія яких відбувається у трьохмірному просторі. Кластери міжвузельних атомів, вакансійні кластери з розміром п'ять та більше вакансій, а також кластери, які складаються з атомів вуглецю та точкових дефектів, розглядаються як нерухомі об'єкти. Вибор параметрів моделі, а саме, значення коефіцієнтів дифузії, енергії формування та енергію зв'язування точкових дефектів та точкових дефектів із атомами вуглецю грунтується на даних експерименту та результатів розрахунків з перших принципів. Деякі параметри моделі були додатково скоректовані незначним чином для досягнення найкращого узгодження даних моделювання методом кластерної динаміки та експериментальних даних щодо впливу ізохронного відпалу на відновлення дефектної структури електронно-опроміненного вольфраму. Експериментальний пік відновлення при температурі 70 К на першої*

стадії у цілому добре відтворюється у моделюванні методом кластерної динаміки як для вольфраму без домішків, так і для вольфраму з вуглецем. Експериментальні піки відновлення на другої стадії відновлення дефектної структури вольфраму формуються, згідно з нашим дослідженням, завдяки взаємодії точкових дефектів та атомів вуглецю.

Ключові слова: відпал, опромінювання, вольфрам, вуглець, кластерна динаміка.

Одержано редакцією 03.09.2017 Прийнято до друку 15.10.2017

УДК 539.3 PACS 02.70

A. D. Petrov

BEHAVIOR OF MATERIAL WITH A MEMORY OF FORM AND PSEUDOELASTICITY UNDER NONSTATIONARY LOADING OF THE BODY

A nonstationary thermo-elastic-plastic problem is examined for pseudoelastic bodies. The key feature of theory consists in that the diagram of tension of deformations appears as a three-unit broken line and can have a falling down segment. Thus the characteristic points of the diagram depend on the material's temperature and phase state. Such character of the diagram leads to the discontinuous *solutions and as a result to the moving boundaries of phase transitions. The example of thin stripe at uniaxonic tension is considered. It is shown that deformation is not homogeneous through the stripe and its development depends on the material's properties. The got results confirm an idea that front of races change of deformation spreads with permanent speed that depends only on mechanical properties of material.*

Keywords: thermo-elastic-plasticity, pseudoelasticity, form memory, phase transitions.

1. Introduction

The list of alloys that exhibit pseudoelasticity includes Ni-Ti alloys and various copper, iron, silver and gold-based alloys. Pseudoelasticity is the ability of a material to accumulate deformations upon loading at a high temperature regime and then return to its original state after unloading (through the hysteresis loop). The mechanism of this reduction is the transformation from the martensite phase to the original austenite phase.

Such alloys as NiTi, CuZnAl, CuAlNi, AuCd and others can restore deformations up to 3%. Important characteristics of some of these materials are internal damping, pseudoelasticity and high yield strength. It is noted that the amount of experimental data of high quality of macroscopic behavior of NiTi remains limited.